

Battery Energy Storage System Economic Benefits Assessment on a Network Frequency Control

Kréhi Serge Agbli, Samuel Portebos, Michaël Salomon

Abstract—Here a methodology is considered aiming at evaluating the economic benefit of the provision of a primary frequency control unit using a Battery Energy Storage System (BESS). In this methodology, two control types (basic and hysteresis) are implemented and the corresponding minimum energy storage system power allowing to maintain the frequency drop inside a given threshold under a given contingency is identified and compared using DigSilent's PowerFactory software. Following this step, the corresponding energy storage capacity (in MWh) is calculated. As PowerFactory is dedicated to dynamic simulation for transient analysis, a first order model related to the IEEE 9 bus grid used for the analysis under PowerFactory is characterized and implemented on MATLAB-Simulink. Primary frequency control is simulated using the two control types over one-month grid's frequency deviation data on this Simulink model. This simulation results in the energy throughput both basic and hysteresis BESSs. It emerges that the 15 minutes operation band of the battery capacity allocated to frequency control is sufficient under the considered disturbances. A sensitivity analysis on the width of the control deadband is then performed for the two control types. The deadband width variation leads to an identical sizing with the hysteresis control showing a better frequency control at the cost of a higher delivered throughput compared to the basic control. An economic analysis comparing the cost of the sized BESS to the potential revenues is then performed.

Keywords—Battery Energy Storage System, electrical network frequency stability, frequency control unit, PowerFactory.

I. INTRODUCTION

THE AC power systems stability is a main issue affecting power system operation, security, reliability and efficiency. Power system stability is threefold: rotor angle stability, voltage stability and frequency stability. The rotor angle stability is seen as a local imbalance issue of the synchronous generations' units in the electrical grid whereas voltage stability is analyzed regarding the balance between produced and consumed reactive power in every node of the network. The rotor angle stability is considered during network design or expansion whereas the frequency and the voltage stabilities are a continuous issue to pay attention to during the operation of the electricity grid [1]-[6].

The power generation and consumption must continuously match in order to avoid frequency deviations from the nominal value. However, as both consumption and generation continuously vary, a proper frequency control of the network

is necessary. This topic becomes even more prevalent with the uptake of renewables, which may cause high power imbalances on the network, as well as reduce the contribution to the frequency control of the conventional units they replace. The frequency control principle is based on several actions gathered in four control loops: primary, secondary, tertiary and emergency controls in a timeline of hundreds of milliseconds up to minutes [7].

In Europe, BESS-based frequency response is performed by around 1,004 MW of batteries; in North America the batteries capacity is at about 779 MW and 233 MW in Australia and Oceania whereas in Asia the batteries capacity is up to around 625 MW gathering only operation projects [8]. BESS participation to the frequency control is increasingly growing mainly due to the reduction in investment cost, which makes BESS competitive for those services compared to more conventional generation sources (such as thermal, hydroelectric or nuclear power plants).

The main constraint in primary frequency control is the necessity of a quick response in order to avoid frequency drops reaching a Nadir out of the allowed thresholds in a timeline of hundreds of milliseconds up to a few seconds. The increased penetration of intermittent renewables tends to decrease the total inertia of electrical networks leading to an increased need in ultra-fast response [3], [4], [9]. In this context, BESS-based power system is one of the alternatives allowing to provide fast primary frequency control thereby reinforcing the stability of the network. The frequency control unit power response is proportional to the frequency deviation value with a deadband in which no control action is performed. Several methods to implement primary frequency control are compared based on South Africa's grid code requirement, the frequency control unit set-point's transmission time step-size and time lag, and the data acquisition time lag. Based on these constraints, several works emphasizing on primary frequency control based on BESS have been done [10]. The common basic primary control principle encompasses one or two of the following terms according to whether or not the control unit is based on BESS: the regulating power, proportional to the frequency deviations, and an offset term computed to manage the BESS State-of-Energy (SOE) [7], [9], [11]-[14].

In this paper, techno-economic analysis is performed on both basic primary frequency control principle commonly found in the literature and a variant including a hysteresis component intending to enhance the quality of the frequency response. The analysis also aims at evaluating the economic impact of both primary frequency control principles.

Kréhi Serge Agbli, Ph.D., is with the Research and Development, Clean Horizon Consulting, Paris, France (phone: 0033-768-0373; e-mail: aks@cleanhorizon.com).

Samuel Portebos, M.Sc. Head of Engineering, and Michaël Salomon, Ph.D., CEO, are with the Clean Horizon Consulting, Paris, France (e-mail: sp@cleanhorizon.com, ms@cleanhorizon.com).

First, the considered methodology of the economic benefit of both approaches will be highlighted, then the related simulation results obtained on IEEE 9 bus model under PowerFactory will be brought out. The storage assets sizing versus the annualized investing and operating cost will be provided with analysis on the business model in which the method with the best frequency response quality could be deployed.

II. METHODOLOGY OF ECONOMIC BENEFIT ASSESSMENT OF BESS ASSET DEDICATED TO PRIMARY FREQUENCY CONTROL

The main objective of this research is to determine whether BESS-based frequency control units can be technically suited and economically viable compared to more conventional alternatives. The battery-based primary control units (BESSs) proposed should be able to properly maintain the frequency of the grid within the allowed thresholds following a drop due to

the occurrence of a given contingency. The variable of the sizing exercise is at first the power rating of the BESS, as, over these short-term simulations, the impact on the energy rating is disregarded. Indeed, the used energy to deal with a contingency is negligible compared to the useful energy of typical batteries designed to maintain the nominal charge or discharge power rating during at least 15-min whereas the frequency setpoint is reached over a few seconds (5-30s). Based on these results, and depending on the dead-band scenario considered, the BESS representing the lowest cost will be identified as the best solution. Moreover, the impact of the BESS' operation over a long-term frequency control period (monthly or yearly scale) on the energy rating will also be considered in the economic analysis. The techno-economic analysis methodology to assess the sizing in terms of both power rating and energy rating of the BESS and the corresponding cost is summarized in Fig. 1.

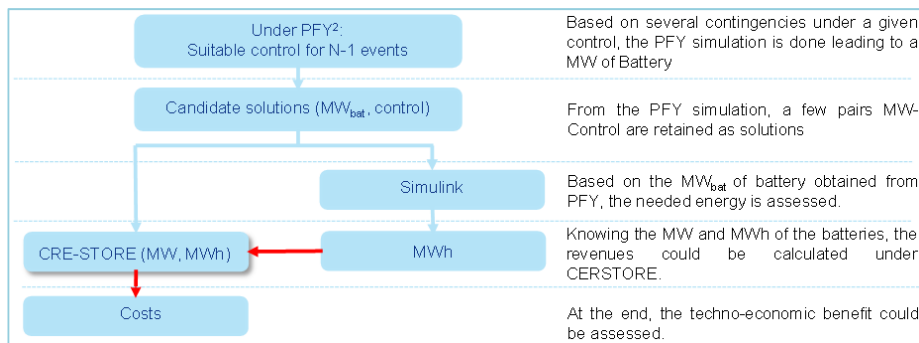


Fig. 1 The techno-economic analysis methodology to assess the revenues and the capacity of the battery

As depicted in Fig. 1, the first step consists of defining a contingency and identifying the minimum BESS power rating allowing to alleviate the impact of the contingency and maintain the frequency within an acceptable range. Then, the proper frequency control method paired to the identified minimum battery power rating is considered as a candidate solution.

Next, the energy rating of the storage system is assessed in order to calculate the investment cost. This is done through a dedicated Simulink model. Indeed, the PowerFactory model is dedicated to performing transient analysis of the grid with a timescale of a dozen seconds. Therefore, to assess the MWh-capacity based on long duration data (over a period of several hours with around 1s time-step), a Simulink model is used since the quasi-dynamic simulation of PowerFactory only covers a 15-min time-step simulation with steady-state calculation, which is insufficient for the long-term impact on the sizing being assessed.

Finally, knowing the MW/MWh capacity of the storage system, the project cost can accurately be assessed, allowing to compare the candidate solutions and identify the least costly one.

The aforementioned methodology will be followed considering two BESS strategies. The first strategy is the basic BESS developed in PowerFactory and available as "Template"

in PowerFactory library. The second one is the hysteresis BESS developed by Clean Horizon Consulting.

A. The Frequency Control Principles and the Considered Hypotheses to Underlie the Study

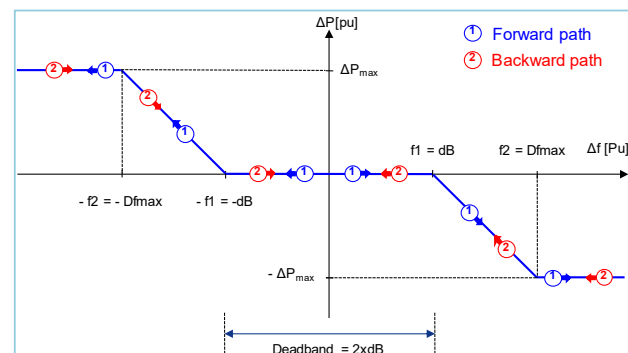


Fig. 2 Frequency control principles indicating basic approach in the Powerfactory Template (Basic BESS principle)

The two frequency control principles to be integrated in the BESS are presented in the following. Fig. 2 highlights the basic frequency control principle where the power set-point of the storage unit is fixed based on the frequency deviation with an inactive deadband. The power set-point follows the same

path regardless of the frequency deviation direction: forward trend when dropping or backward trend under control action (Fig. 2).

Contrary to the previous case, the hysteresis BESS principle is depicted on Fig. 3. Whenever the frequency deviation is higher than the maximum value Df_{max} (in absolute value) at which the maximal power of the storage unit is delivered, forward and backward paths are the same. Whenever the frequency deviation is lower than Df_{max} , the backward path follows another path, mimicking a hysteresis (Fig. 3).

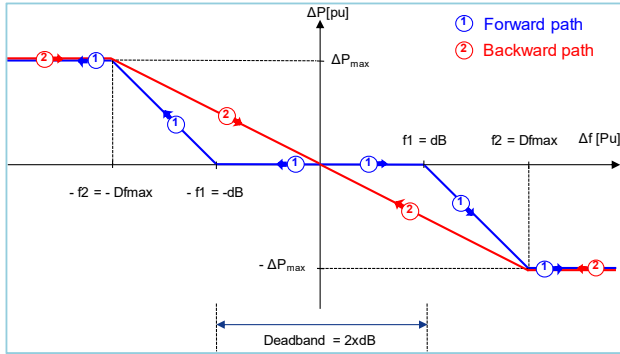


Fig. 3 Frequency control principles indicating hysteresis approach in the Clean Horizon Consulting model (BESS hysteresis): when frequency drop Nadir is lower than Df_{max} at which the available entire BESS capacity is activated

In the case the frequency deviation does not reach Df_{max} , the backward path of the hysteresis is depicted on Fig. 4 (path 2 in red). This backward trend avoids a sharp raise of the frequency. During the backward path, the last power set-point value in the forward path remains the maximum allowable set-point on the backward path (Fig. 4).

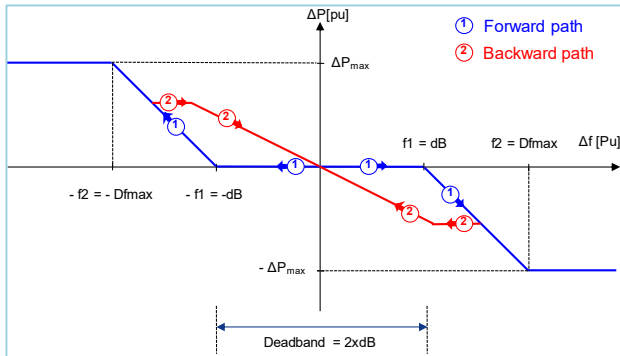


Fig. 4 Frequency control principles indicating hysteresis approach in the Clean Horizon Consulting model (BESS hysteresis): when frequency drop Nadir is lower than Df_{max} at which the available entire BESS capacity is activated

The BESS has the ability to provide whether active or reactive power assistance either to perform frequency control or voltage control according to (1):

$$\begin{cases} I_{qin} = f(K_f \cdot \Delta f) \\ I_{pin} = K_v \cdot \Delta V \end{cases} \quad (1)$$

The voltage control assistance is here neglected by tuning the related control parameter K_v to a null value.

The control block receives both active and reactive current inputs (I_{pin} and I_{qin}) with a priority flag indicating whether an active power control priority or reactive power control one. Therefore, when reactive power control priority is ongoing, the reactive current (I_{qcmd}) is going to vary between $-I_{max}$ and I_{max} limiting therefore the current value of the active current output. Whenever the active power control priority is allowed, the active current output (I_{pcmd}) varies from 0 to I_{max} , limiting thereby the value of the reactive current as indicated by (2) and (3) [6]:

$$\begin{cases} I_{qcmd} = \lim(I_{qin}, I_{qmin}, I_{qmax}) \\ I_{pcmd} = \lim(I_{pin}, I_{pmin}, I_{pmax}) \end{cases} \quad (2)$$

$$\begin{cases} I_{pcmd} = \text{if } Q \text{ priority } PQflag = 0 : \begin{cases} I_{qmax} = I_{max} \\ I_{qmin} = -I_{min} \\ I_{pmax} = \sqrt{I_{max}^2 - I_{qcmd}^2} \\ I_{pmin} = 0 \end{cases} \\ I_{qcmd} = \text{if } Q \text{ priority } PQflag = 1 : \begin{cases} I_{pmax} = I_{max} \\ I_{pmin} = 0 \\ I_{qmax} = \sqrt{I_{max}^2 - I_{pcmd}^2} \\ I_{qmin} = -\sqrt{I_{max}^2 - I_{pcmd}^2} \end{cases} \end{cases} \quad (3)$$

The two frequency control principles (basic and hysteresis) are implemented in DSL (DIGSILENT Simulation Language). Those two models only differ by the respective block definitions in the linked common models: The corresponding frequency control method is implemented in each block definition model (basic of Fig. 2 and the hysteresis frequency control of Figs. 3 and 4) (Fig. 5).

The state transition diagram of the Basic BESS principle is provided in Fig. 6 to summarize the basic principle block definition of Fig. 5:

- Transitions 0.1 or 0.4 from start state: frequency deviation ($\Delta f = f - f_0$) could be negative whenever the frequency drops down or positive in case the frequency rises above the reference frequency f_0 . Transition 0.1 occurs if Δf is negative and 0.4 when positive. In the following description, from the start state, it is considered the 0.1 transition where the frequency is in the negative part of the deadband.
- Transition 1.1: when the frequency drops outside the deadband, the frequency control follows the forward path of Fig. 2 until to reach the maximum available frequency control asset power at $-f_2$ (Fig. 2).
- Transition 2.1: If the frequency control action starts increasing, the frequency goes back toward the reference value f_0 , the control follows the same control path according to the Fig. 2.
- Transition 4: If the frequency increases above the

reference value f_0 , the control enters the positive deadband area (Fig. 2).

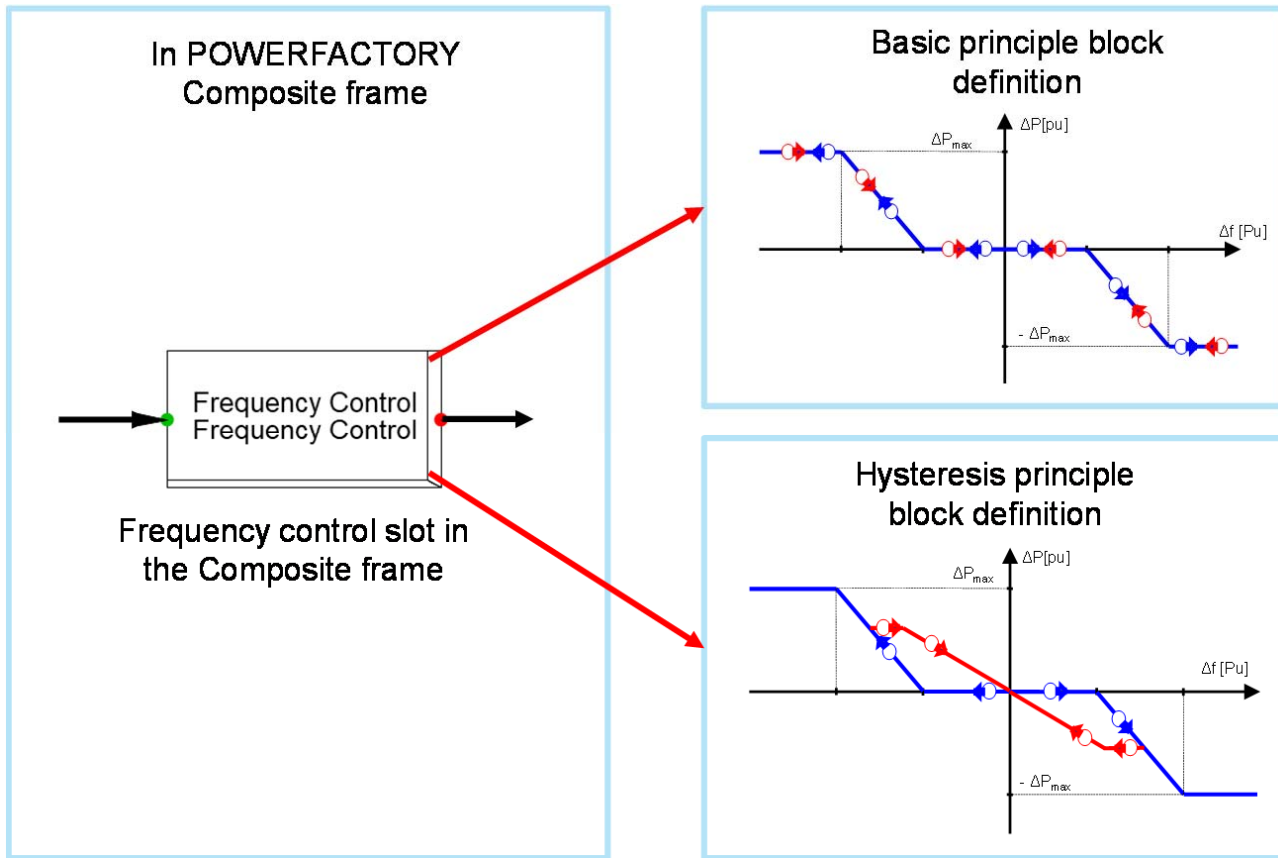


Fig. 5 Both frequency control principles in the composite frame

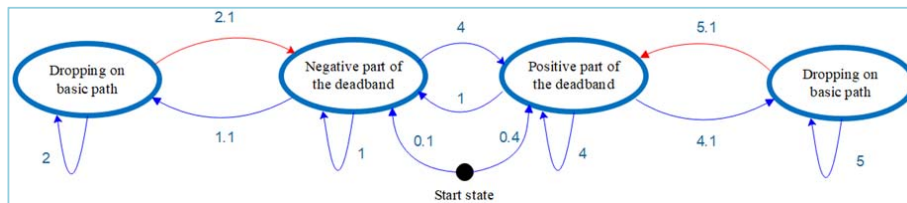


Fig. 6 State Transition Diagram (Basic BESS principle)

The basic BESS principle reversely follows the same control in the positive area where the frequency deviation remains positive.

The state transition diagram of the hysteresis BESS principle in Fig. 7 summarizes the hysteresis principle block definition of Fig. 5. The only difference being the control under hysteresis path when the frequency is brought back toward the reference value (Fig. 7).

- Transition 3.1: If the frequency control action starts increasing, the frequency goes back toward the reference value f_0 , the control follows the hysteresis control path (backward path) according to Figs. 3 and 4.
- Transition 3.2: If the frequency control action drops anew before having moved in the positive part of the deadband,

the hysteresis path (backward path) is followed by the control (Figs. 3 and 4).

- Transition 4: If the frequency increases above the reference value f_0 , the frequency control action enters the positive deadband area (Figs. 3 and Fig. 4).

The positive part of the diagram is also the reverse control principle of the negative part.

III. SIMULATIONS UNDER POWERFACTORY TO ASSESS THE BATTERY POWER NEEDED FOR BOTH BESS

The PowerFactory model is performed based on IEEE 9 Bus bar model available in [15], [16]. Three BESS-based subsystems have been integrated to this grid as shown in Fig.

The N-1 contingency retained to assess the support effect of each kind of frequency control principle (basic and hysteresis) is the tripping of the generator G2 (270 MVA).

```

graph LR
    Start((Start state)) -- 0.1 --> NP[Negative part of the deadband]
    NP -- 1 --> NP
    NP -- 0.4 --> PP[Positive part of the deadband]
    PP -- 1 --> NP
    PP -- 4 --> PP
    NP -- 3.1 --> HP1[Hysteresis path]
    HP1 -- 3.2 --> NP
    HP1 -- 3 --> HP1
    PP -- 6.1 --> HP2[Hysteresis path]
    HP2 -- 6.2 --> PP
    HP2 -- 6 --> HP2
    NP -- 1.1 --> DB1[Dropping on basic path]
    DB1 -- 2 --> DB1
    DB1 -- 2.1 --> HP1
    PP -- 4.1 --> DB2[Dropping on basic path]
    DB2 -- 5 --> DB2
    DB2 -- 5.1 --> HP2
  
```

The schematic diagram illustrates the power system configuration, showing the interconnection of various components:

- Generators:**
 - Generator 1:** 512 MVA, connected to Bus 10.
 - Generator 2:** 270 MVA, connected to Bus 2.
- Buses:** The system includes Buses 1 through 11, each represented by a square symbol. Buses are color-coded: blue (Buses 2, 7), green (Buses 8, 9, 11), yellow (Buses 5, 6), and red (Buses 1, 4, 10).
- Transformers:** Labeled T1 through T5, shown as circles with two windings.
 - T1 connects Bus 10 to Bus 1.
 - T2 connects Bus 2 to Bus 7.
 - T3 connects Bus 9 to Bus 3.
 - T4 connects Bus 10 to Bus 1.
 - T5 connects Bus 11 to Bus 3.
- Lines:** Transmission lines connect the buses:
 - Line 1: Red line connecting Bus 4 to Bus 10.
 - Line 2: Blue line connecting Bus 2 to Bus 7.
 - Line 3: Blue line connecting Bus 7 to Bus 8.
 - Line 4: Green line connecting Bus 8 to Bus 9.
 - Line 5: Green line connecting Bus 9 to Bus 6.
 - Line 6: Yellow line connecting Bus 6 to Bus 5.
- Loads:** Represented by triangle symbols.
 - Load A:** Connected to Bus 5.
 - Load B:** Two locations, one connected to Bus 8 and another to Bus 6.
- Interconnections and BESS:**
 - A connection labeled "C" links the bus area around Bus 8 to the bus area around Bus 6.
 - The bus area around Bus 6 is connected to the **BBESS PCC**.
 - The **BBESS PCC** is connected to three BESS units:
 - Hysteresis BESS:** Consists of BAT BESS CHC, LV, and BAT BESS PF.
 - Basic BESS:** Consists of BB EVO1 and BESS CHC/EVO1.

Fig. 8 Single Line Diagram of the IEEE 9 Bus System

A. Small Deadband Configuration

The small deadband configuration considers the following parameters for the frequency control:

- $\text{dB} = 10 \text{ mHz}$
- $f_1 = 10 \text{ mHz}$
- $f_2 = 210 \text{ mHz}$

By tripping the generator G2 at 5 s, the frequency drop based on the two kinds of control principle is plotted together with the battery power profile (Fig. 7).

The steady state frequency deviation (in absolute value) remains out of the deadband and lower than Dfmax . Both BESS types lead to the same battery size and the same Nadir (49.19 Hz). A 62.5 MVA battery system, for both control approaches, is needed to sustain the frequency drop at 49.19 Hz Nadir.

When steady state frequency deviation is greater than Dfmax :

- The backward hysteresis path cannot be followed since

the frequency remains too low.

When steady state frequency deviation is lower than Dfmax :

- Backward frequency response is better for hysteresis path. It emerges therefore that:

- Both BESS have the same sizing results.
- Pbat (basic and hysteresis) = 62.5 MVA.
- Hysteresis BESS leads to a slightly better frequency control than the basic one.

B. Large Deadband Configuration

The large deadband configuration considers the following parameters for the frequency control:

- $\text{dB} = 200 \text{ mHz}$
- $f_1 = 200 \text{ mHz}$
- $f_2 = 400 \text{ mHz}$

By tripping the generator G2 at 5 s, the frequency drop based on the two kind of control principle is going to be plotted as well as the battery power profile (Fig. 8).

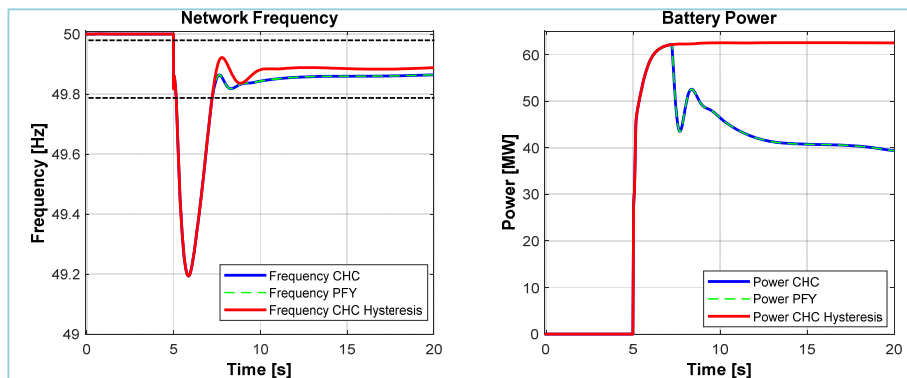


Fig. 9 Small deadband (deadband = 10 mHz and $\text{dfmax} = 210 \text{ mHz}$) configuration with frequency deviation reduced below than dfmax

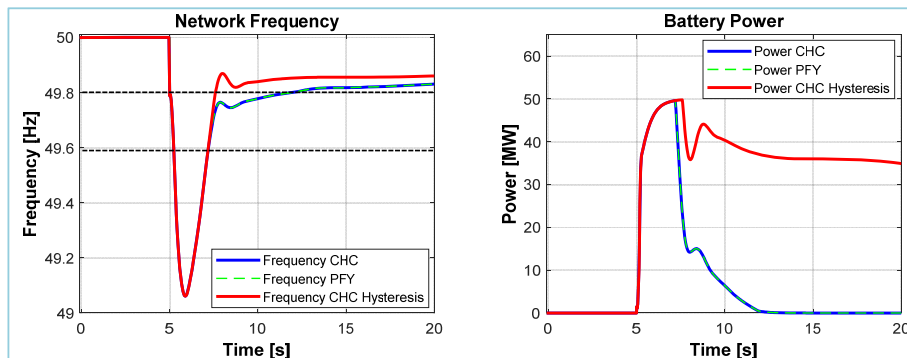


Fig. 10 Large deadband (deadband = 200 mHz and $\text{dfmax} = 400 \text{ mHz}$) configuration at the same battery power for both BESSs

The steady state frequency deviation (in absolute value) is brought back within the deadband. Both BESS types lead to the same battery size and the same Nadir. The basic BESS-based battery power set-point comes back to zero, contrary to that of the hysteresis BESS.

The hysteresis BESS enhances the frequency control compared to the basic BESS when considering an identical BESS sizing. The needed energy throughput is however higher with hysteresis BESS than with the Basic one, as shown in the next section.

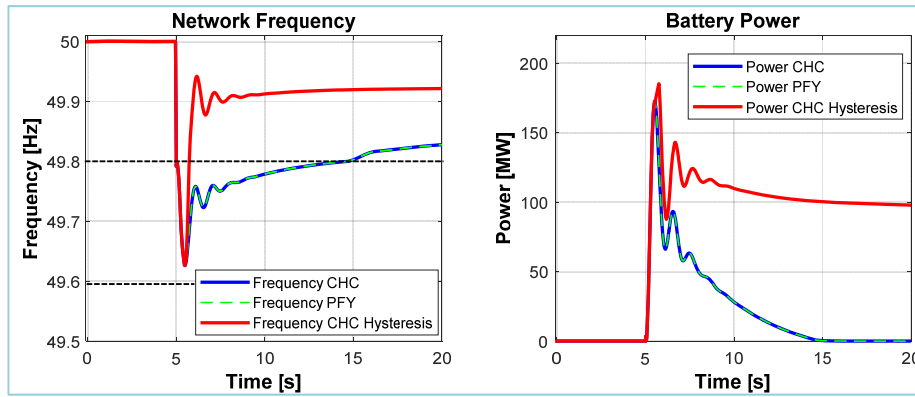


Fig. 11 Large deadband (deadband = 200 mHz and dfmax = 400 mHz) configuration leading to the same Nadir

IV. SIMULATIONS UNDER MATLAB-SIMULINK TO ASSESS THE BATTERY CAPACITY NEEDED FOR BOTH BESS

Both the basic- and hysteresis-based BESSs Simulink models synopsis graph is highlighted below. Because the BESSs alone do not affect significantly a strong grid (high inertia) frequency, the open loop model is relevant to analyze the impact of the two BESSs on the energy rating sizing when considering a high inertia continental network.

- The basic and hysteresis Simulink models contain the same behavior as the one implemented in PowerFactory (the same basic and hysteresis principles).
- Both models are simulated based on the same frequency deviation data.
- The smallest capacity allowing to maintain the frequency in the minimum and maximum bounds is retained.

We consider a standard capacity allocation constraint as it could be required by a typical grid operator. The maximum storage capacity related to the operation band is 15-min (Fig. 10). The needed storage capacity for BESS-based primary control will be calculated in the 15-min threshold. Whenever the required storage system throughput energy will be lower than the 15-min storage capacity allocated to primary frequency control, 1-h capacity will be considered at a given

power (Fig. 10); contrariwise, the storage capacity will be four times the throughput assessed energy.

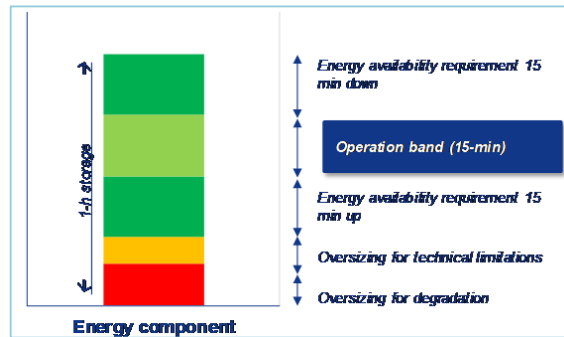


Fig. 12 Energy storage asset operation band assumption

A. SIMULINK-Based Battery Capacity (MWh) Assessment: High Inertia Continental Network

Both basic- and hysteresis-based BESSs Simulink models synopsis graph are presented below. Because the BESSs alone do not significantly affect a large grid's frequency, the open loop model is relevant to compare the two BESSs impact considering a high inertia continental network.

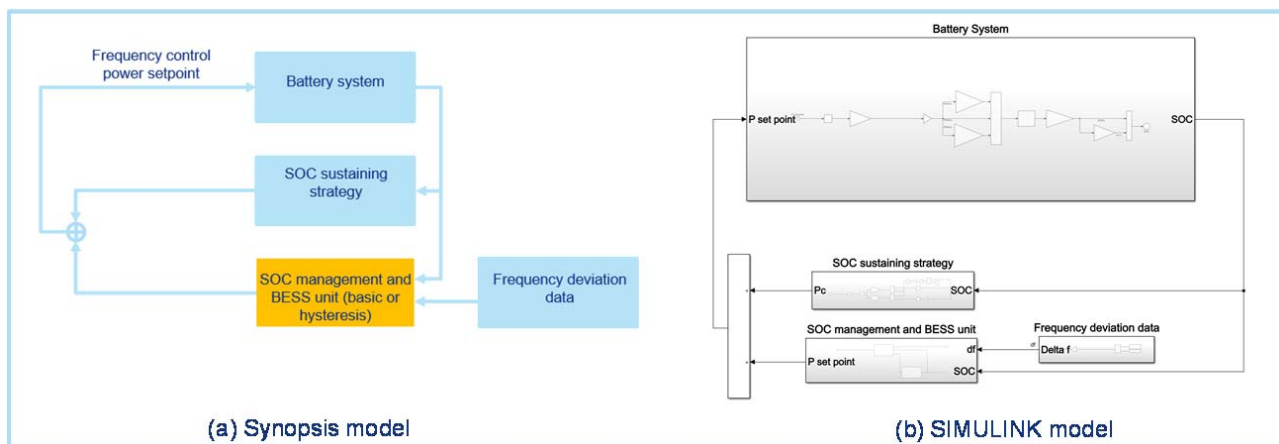


Fig. 13 High inertia continental network in which the BESS participate in the frequency control for both BESSs

Fig. 13 (a) shows the synopsis model and the related Simulink model is provided by Fig. 13 (b). The battery system considered has a power of 62.5 MVA as indicated earlier. The frequency deviation data are plotted in Fig. 14.

We consider a simulation over one-month and deduce that the related capacity could be representative of the overall sizing of the storage unit. The results are scaled up to one-year analysis. The BESS SOC is also plotted in Fig. 14.

Considering small deadband results, it emerges that:

- 15-min storage capacity is enough for both basic and hysteresis BESSs.
- The amount of energy discharged by basic BESS is 216 MWh whereas that of the hysteresis BESS is 366 MWh. This result corresponds to the expected behavior that the hysteresis BESS leads to a higher energy throughput than basic BESS.

The two BESSs therefore lead to the same capacity since the 15-min storage asset) is sufficient enough for both deadbands and both BESSs (only considering the operation band energy component):

- 62.5 MW battery system power.
- 15-min storage capacity allocated to operation band dedicated to primary frequency control.

B. SIMULINK-Based Battery Capacity (MWh) Assessment: Low Inertia Microgrid Network

Both the Basic- and hysteresis-based BESSs Simulink models synopsis graph are provided. The grid model has been integrated leading to a closed loop model. The BESS action therefore affects the grid frequency. This behavior corresponds to that of a microgrid with low inertia, where BESS is the main control device.

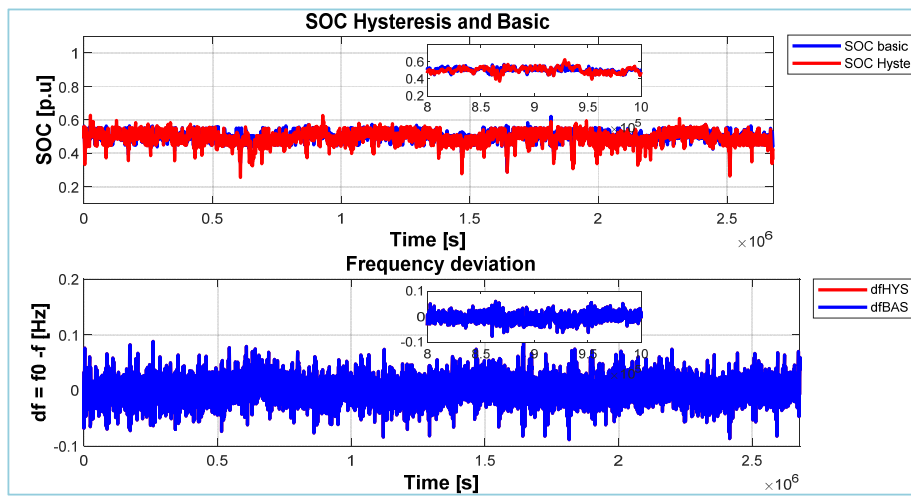


Fig. 14 Small deadband-based simulation: SOC of the battery under both basic and hysteresis BESS for 15-min storage

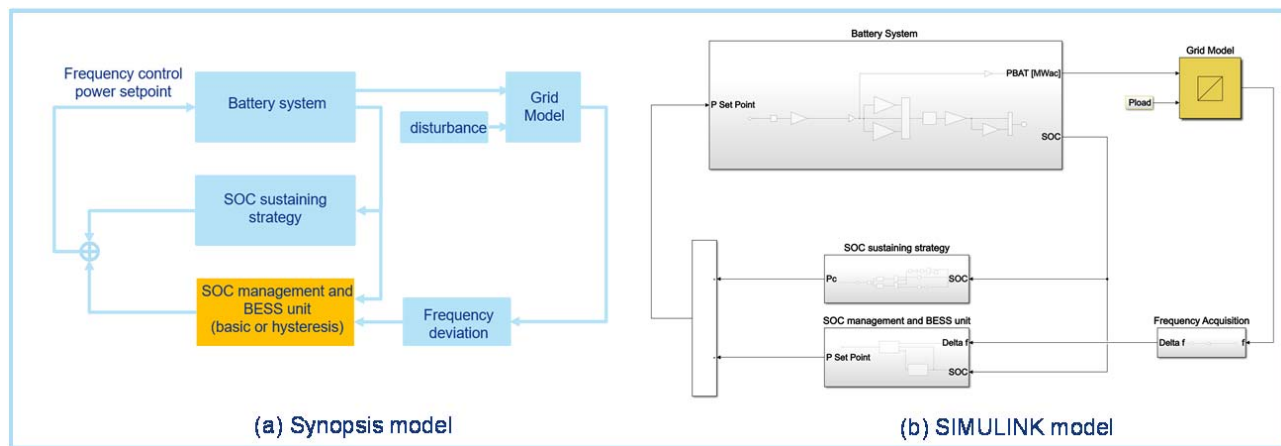


Fig. 15 Low inertia microgrid in which the BESS participate in the frequency control for both BESSs

Fig. 15 (a) presents the synopsis model and the related Simulink model is provided by Fig. 15 (b). The battery system considered has a power of 62.5 MVA, as previously considered.

In order to assess the impact of both BESS control units on the grid's frequency under Simulink simulation, the grid model should be considered under Simulink. The first order grid model presented below [3], [4], [17] is integrated in the

Simulink models simulated.

1) The Grid Model and Its Parameters' Identification Process

The first-order grid model is configured based on the PowerFactory electrical network. The grid equation (Fig. 16) and the parameters identification are summarized in the following.

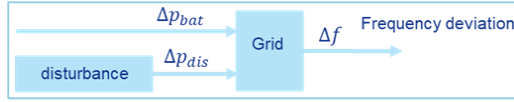


Fig. 16 Low inertia microgrid in which the BESS participate in the frequency control for both BESSs

The frequency deviation first order model of the grid implemented under Simulink is as follows [3], [4]:

$$\Delta f = \frac{\frac{1}{k \cdot s_n}}{\frac{2H}{k f_0} s + 1} \cdot \Delta p = \frac{K}{\tau \cdot s + 1} \cdot \Delta p \quad (1)$$

where $\Delta p = \Delta p_{bat} - \Delta p_{dis}$, Δp_{bat} the battery power in MW, Δp_{dis} the load sudden variation power in MW.

The grid parameters identification is done by the way of three steps. First, in steady state, the parameter k could be assessed as:

$$k = \frac{\Delta p}{\Delta f \cdot s_n} \cdot \Delta p \quad (2)$$

The second step determines the network inertia through the

formula:

$$H = \frac{\sum_i s_{ni} \cdot H_i}{s_n} \quad (3)$$

Finally, by running the PowerFactory model considering 50% of incremental load increase, Δp and Δf are measured.

TABLE I
GRID DYNAMIC CHARACTERISTICS

Grid characterization	
Δp [MW]	157.5
Δf [Hz]	0.38936
k	0.4460

These parameters are identified from the 62.5 MVA BESS-based grid in PowerFactory environment. The obtained parameters are used to configure the Simulink model.

2) The BESSs Impact on the Frequency Deviation and the Battery SOC's Time Series Results

Only the battery capacity necessary to deal with the frequency regulation is considered. The State of Charge is therefore allowed to vary from 0.05 to 0.95. The related assessed battery capacity will therefore be the intrinsic capacity dedicated to frequency regulation related to the operation band energy component, as stated before.

The simulation is performed based on one-month cycle disturbance data. Thence, the needed energy capacity representative of the overall sizing of the storage unit is deduced. The results are scaled up to one-year analysis. The BESS SOC is also plotted on Fig. 17.

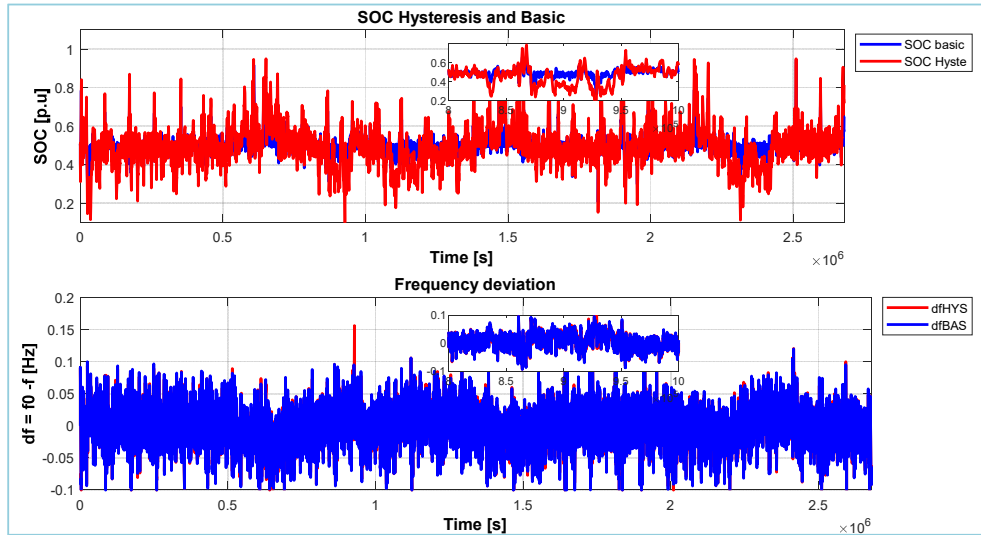


Fig. 17 Small deadband-based simulation: SOC of the battery under both basic and hysteresis BESS for 15-min storage

The closed loop simulation roughly leads to the same conclusion.

Considering small deadband results, it emerges that:

- o 15-min storage capacity is enough for both basic and hysteresis BESSs.

- o The amount of energy discharged by the basic BESS throughput is 365 MWh whereas that of the hysteresis BESS is 431 MWh. This result corresponds to the expected behavior the hysteresis BESS leads to a higher energy throughput than basic BESS.

The two BESSs therefore lead to the same capacity since

the 15-min storage asset (only operation band energy component) is sufficient for both deadbands and both BESSs:

- 62.5 MW battery system power.
- 15-min storage capacity allocated to operation band dedicated to primary frequency control.

From this analysis based on Basic and hysteresis BESS dedicated to primary frequency control, the simulations based on the small deadband needing more throughput energy from the BESS leads to the same sizing for both Basic and hysteresis BESS. However, the hysteresis BESS provides a better frequency control maintaining the resulting regulated frequency closer to the reference value (50 Hz).

V. STORAGE ASSETS SIZE VERSUS THE ANNUALIZED INVESTING AND OPERATING COST

In this section, the investment cost of the BESS system is assessed based on the assumptions in Fig. 18. As said earlier, the hysteresis BESS requires more energy than basic one, however the 15-min storage dedicated to frequency control is sufficient for the hysteresis control principle as it is for the basic control principle. Therefore, the 1-h storage capacity is considered for both frequency control principles (Fig. 12).

Financing hypothesis	
Business case duration (years)	15
Actualization rate (in %)	6%
Financing hypothesis Battery	
Cost power component (€/kW)	150
Cost Energy component (€/kWh)	250
Fixed cost (Design and Engineering)(0.5% Capex or k€)	300
Cost of module repowering (€/kWh)-10Years	150
Opex (% capex or k€)	100
Project size Bat	
BAT Power(MW)	50
Storage hours	1
Bat Efficiency	92%

Fig. 18 BESS business case hypotheses

Based on the assumptions of Fig. 18, the annualized cost (4) of the BESS is assessed. The Levelized Cost of Energy is also calculated by extrapolating the results over the lifetime of the BESS (5).

$$Cost_{Annualized} = \sum_{i=0}^n \frac{C_i}{(1+r)^i} \quad (4)$$

$$LCOS = \frac{Cost_{Annualized}}{\sum_{i=1}^n \frac{E_i}{(1+r)^i}} \quad (5)$$

where: C_i the spent cost in year i , r is the actualization rate, E_i is the throughput energy in year i .

A. Annualized Cost of the Battery Asset: High Inertia Continental Grid and Low Inertia Microgrid

It appears from Fig. 19 that, if any annualized new investment cost of a conventional thermal assets is higher than 25.46 M€, the hysteresis BESS is a more economical investment.

Components of the costs for small dead band study case based on the Hysteresis energy injected on the grid (M€)

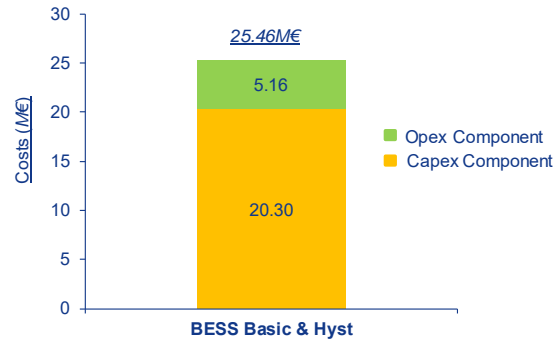


Fig. 19 Components of the costs for small deadband study case based on the Hysteresis energy injected on the grid (M€)

B. The Study Case in Favor of the Hysteresis BESS System

In the case of renewables penetration, the requirement of power reserve for frequency containment may be necessary. If investment in new assets is required, the BESS system could be preferable to conventional solution.

In a low inertia microgrid with high renewables penetration and potential curtailment of intermittent renewables, the primary frequency control based on hysteresis BESS could be the better option compared to basic frequency control.

VI. CONCLUSION

In order to obtain the sizing of a storage asset dedicated to performing primary frequency control, a methodology is proposed and applied to both basic and hysteresis frequency control based on BESS for small and large deadbands application. Based on N-1 contingency in the PowerFactory environment, the energy storage asset power is identified. Then by considering a given grid disturbance, under MATLAB-Simulink, the needed MWh-capacity of both control approaches (basic and hysteresis) is computed. For a given primary control frequency method, the related storage asset has been sized. Then, the corresponding cost of the solution has been calculated.

Only the annualized cost of the storage asset has been calculated here by lack of real project data for comparison

The proposed methodology could be applied to a given frequency control project to compare different energetic assets for a convenient investment analysis.

APPENDIX

The IEEE 9 bus system example PowerFactory model parameters are made available in [15], [16]. The related energetic devices data are provided hereafter.

TABLE II
GENERATORS

	Synchronous generators		
	G1	G2	G3
Nominal power [MVA]	512	270	125
Voltage [kV]	24	18	15.5
Power factor	0.9	0.85	0.85

TABLE III
TRANSFORMERS

	Transformers		
	TF1	TF2	TF3
Nominal primary voltage	24	18	15.5
Nominal secondary voltage	230	230	230

TABLE IV
LOADS

	Loads		
	A	B	C
Apparent Power [MVA]	125	90	100
Power factor	0	0	0

REFERENCES

- [1] Hassan Bevrani, Qobad Shafiee, Hemin Golpira. Frequency Stability and Control in Smart Grids. IEEE Newsletter, September 2019.
- [2] Zeyad Assi Obaid, Liana M. Cipcigan, Lahieb Abraham, Mazin T. Muhssin. Frequency control of future power systems: reviewing and evaluating challenges and new control methods. J. Mod. Power Syst. Clean Energy (2019) 7(1):9–25. <https://doi.org/10.1007/s40565-018-0441-1>.
- [3] Robert Eriksson, Niklas Modig, Andreas Westberg. FCR-N design of requirements. Entsoe report. 5 July 2017.
- [4] Entsoe. Supporting Document on Technical Requirements for Frequency Containment Reserve Provision in the Nordic Synchronous Area. Prequalification Working Group, FCP project; 26 June 2017.
- [5] Y. Fang et al. A proposed framework for coordinated power system stability control. CIGRE, C2/C4 Technical brochure, Ref 742. ISBN: 978-2-85873-444-3. September 2018. 149 Pages.
- [6] K. Yamashita et al. Modelling of inverter-based generation for power system dynamic studies. CIGRE, Technical Brochure C4/C6/C1RED, Ref 727. ISBN: 978-2-85873-429-0. MAY 2018, 292 Pages.
- [7] Mihai Sanduleac, Lucian Toma, Mircea Eremia, Valentin A. Boicea, Dorian Sidea, Alexandru Mandis. Primary frequency control in a power system with battery energy storage systems. 2018 IEEE International Conference on Environment and Electrical Engineering and 2018 IEEE Industrial and Commercial Power Systems Europe (EEEIC / I&CPS Europe).
- [8] Database CHESS (Clean Horizon' Energy Storage Source). At 15 June 2020.
- [9] Diego Mejía-Giraldo, Gregorio Velásquez-Gomez, Nicolás Muñoz-Galeano, Juan Bernardo Cano-Quintero and Santiago Lemos-Cano. A BESS Sizing Strategy for Primary Frequency Regulation Support of Solar Photovoltaic Plant. Energies 2019, 12, 317.
- [10] Bolun Xu, Alexandre Oudalov, Jan Poland, Andreas Ulbig, Göran Andersson. BESS Control Strategies for Participating in Grid Frequency Regulation. Proceedings of the 19th World Congress the International Federation of Automatic Control. Cape Town, South Africa. August 24-29, 2014.
- [11] Appendix 1: Load-Frequency Control and Performance. Union for the Coordination of the Transmission of Electricity (UCTE). final 1.9 E, 16.06.2004.
- [12] Zhuangxi Tan, Xinran Li, Li He, Yong Li, Jiyuan Huang. Primary frequency control with BESS considering adaptive SoC recovery. Electrical Power and Energy Systems. <https://doi.org/10.1016/j.ijepes.2019.105588>.
- [13] Rijo Rajan, Francis M. Fernandez. Power control strategy of photovoltaic plants for frequency regulation in a hybrid power system. Electrical Power and Energy Systems 110 (2019) 171-183.
- [14] Giacomo-Piero Schiapparelli, Stefano Massucco, Emil Namor, Fabrizio Sossan, Rachid Cherkaoui, Mario Paolone. Quantification of primary frequency control provision from battery energy storage systems connected to active distribution networks. PSCC 2018 Power Systems Computation Conference, At Dublin, Ireland. 7 pages.
- [15] <https://www.kios.ucy.ac.cy/testsystems/index.php/dynamic-ieee-test-systems/ieee-9-bus-modified-test-system>
- [16] JP Bérard. IEEE 9 Bus System Example. OPAL-RT. 23 Oct 2017. 13 Pages.
- [17] Mikko Kuivaniemi, Niklas Modig, Robert Eriksson. FCR-D design of requirements. entsoe report, 5 July 2017.

Kréhi Serge Agbli. After a master's degree in electrical and electronic systems at Felix Houphouët-Boigny University in Abidjan in Côte d'Ivoire, Dr AGBLI obtained his doctorate in electrical engineering at the University of Franche-Comté in France in 2012.

His main research interests include energy systems, renewable energy for stationary and transportation applications, energy storage systems, energy management strategies, energetic hybridization and renewable energies-based micro-grids. He has been involving in several industrial and academic projects which are focused on locomotives, automotive, onshore and offshore micro grid-based renewable energies.

Dr. AGBLI's main task on the R & D axis is the causal / non-causal, static, and / or dynamic, optimal and suboptimal modeling of power grids with a focus on storage integration. He is therefore actively involved in projects relying on Clean Horizon's CRE-STORE simulation tool. In addition, Serge develops models of electrical network under MATLAB-SIMULINK ® or PowerFactory® to execute more detailed stability and transient analyses.

Samuel Portebos. Graduated in engineering at Ecole Centrale de Lille (France) and in electrical engineering at Pontificia Universidade Catolica de Rio de Janeiro (Brazil).

At Clean Horizon, he leads all the company's technical consulting activities, which include identification of the need for energy storage at the local or national level, optimal sizing of energy storage projects, and storage projects due diligence. Samuel has been active on over 40 storage projects in more than 25 countries, representing a volume of more than 700 MWh of storage capacity.

Mr. Portebos has been the main designer of Clean Horizon's CRE-STORE energy storage simulation tool.

Michaël Salomon. Michael obtained his engineer's degree at Mines ParisTech in France and his Ph.D. at Stanford in the USA. He witnessed the booming of cleantech venture capital and entrepreneurship while an academic in the Silicon Valley, and then went on to become a management consultant at McKinsey in Paris.

In 2009, he founded Clean Horizon in Paris which he has led and grown since then. Since its creation, Clean Horizon has confirmed its status as the only, boutique consultancies in the world specialized solely on energy storage.

Clean Horizon is active globally (Europe, Africa, Americas, Asia) both as a market analyst and as a technical consultancy focusing on energy storage. As of 2018, Clean Horizon serves the Caribbean and Latin American markets from its Miami subsidiary, Clean Horizon Americas, of which Michael is the President.